

# The role of theta and gamma oscillations in item memory, source memory, and memory confidence

Syanah C. Wynn<sup>1,2,3</sup>  | Christopher D. Townsend<sup>3</sup>  | Erika Nyhus<sup>2</sup> 

<sup>1</sup>Neuroimaging Center, Johannes Gutenberg University Medical Center Mainz, Mainz, Germany

<sup>2</sup>Department of Psychology and Program in Neuroscience, Bowdoin College, Brunswick, Maine, USA

<sup>3</sup>Centre for Human Brain Health, School of Psychology, University of Birmingham, Birmingham, UK

## Correspondence

Syanah C. Wynn, Neuroimaging Center, Johannes Gutenberg University Medical Center Mainz, Mainz, Germany.  
Email: [wynnsyan@uni-mainz.de](mailto:wynnsyan@uni-mainz.de)

## Funding information

Clinical Center, Grant/Award Number: R15MH114190

## Abstract

Theta and gamma oscillations have been linked to episodic memory processes in various studies. Both oscillations seem to be vital for processes guided by the medial temporal lobe, such as the retrieval of information from memory. While theta oscillations increase with successful memory, it is unclear what the unique contribution of theta is to various subcomponents of memory. On the other hand, memory-related gamma oscillations have been mainly reported in the hippocampus, leaving the role of neocortical gamma in memory underexplored. In this study, we investigated how unique variability in memory accuracy and memory confidence contributes to fluctuations in theta and gamma power. To this end, we recorded EEG from 54 participants while they performed a source memory task. From this task we obtained their item memory accuracy, source memory accuracy, item memory confidence, and source memory confidence. These behavioral measures were put in a trial-by-trial linear mixed effects model to uncover their unique contribution to the oscillatory power in frontal and parietal regions. Our results are in line with the involvement of theta oscillations in both memory accuracy and confidence, but seem to indicate a main role for theta oscillations in memory-related confidence. In addition, we found that gamma oscillations play various roles in memory processing, dependent on brain region.

## KEYWORDS

brain oscillations, confidence, EEG, episodic memory, recognition

## 1 | INTRODUCTION

Research into episodic memory, the memory for events that are linked to a specific time and place, frequently looks at two specific subcomponents, referred to as “item memory” and “source memory”. Here, item memory reflects memories for specific and unconnected items, whereas source memory represents associative memories that are

embedded in a context or encoding source. These two components can be seen as two variants of objective memory accuracy, as item and source memory are often classified as either correct or incorrect. On the other hand, the term “memory confidence” is used to reflect the subjective feeling of confidence we have in a recalled memory. Often this is a graded measure and is correlated with the quality and amount of information retrieved. Memory confidence can

This is an open access article under the terms of the [Creative Commons Attribution](https://creativecommons.org/licenses/by/4.0/) License, which permits use, distribution and reproduction in any medium, provided the original work is properly cited.

© 2024 The Authors. *Psychophysiology* published by Wiley Periodicals LLC on behalf of Society for Psychophysiological Research.

be measured in addition to the objective item or source memory performance, to quantify the subjective quality of the memory. When exploring the neural underpinnings of episodic memory in general, research points toward theta and gamma oscillations playing a major role in objective and subjective memory retrieval (Griffiths et al., 2021; Herweg et al., 2020; Jensen et al., 2007; Lega et al., 2016; Nyhus & Curran, 2010; Staudigl & Hanslmayr, 2013). Given the established involvement of these oscillations, it warrants taking a closer look at the specific role they play in memory accuracy and confidence.

Theta (3–7 Hz) oscillations may be vital to several memory-related processes carried out in the medial temporal lobe (MTL), the main hub for episodic memory. For example, theta in the MTL appears to be important for creating temporal associations between elements, grouping them in one episodic event in memory (Herweg et al., 2020). Theta in neocortical areas, which can be recorded with electroencephalography (EEG) and magnetoencephalography (MEG), has also been linked to memory. Specifically, theta power is higher when items are remembered (hits), as compared to either forgotten (misses) or correctly identified as new (correct rejections) (Chrastil et al., 2022; Duzel et al., 2003, 2005; Wynn et al., 2019, 2020). Similar to the role of theta in the MTL, there is a fairly consistent pattern of cortical theta power increasing when extra associative information is recalled (Addante et al., 2011; Gruber et al., 2008; Guderian & Duzel, 2005; Herweg et al., 2016). In addition, it has been shown that theta power is positively correlated with memory confidence (Wynn et al., 2019, 2020). When looking at these findings, it appears that theta power is involved in the recollection of items, and that this interacts with the associative information and subjectively perceived confidence associated with that item. However, as these memory processes are correlated, it is unclear what their unique relationship with theta oscillations is.

In addition to theta frequency band, gamma (30–50 Hz) oscillations have been proposed to play an important role in memory. For instance, there is a close association between hippocampal gamma and neocortical oscillations during both memory encoding and retrieval (Griffiths et al., 2019; Griffiths & Jensen, 2023; Hanslmayr et al., 2016; Pacheco Estefan et al., 2019). The involvement of gamma in memory encoding appears to be mainly through theta–gamma phase amplitude coupling (PAC). Specifically, it has been proposed that each gamma cycle represents a memory specific representation, which are superimposed onto different phases of the theta cycle, forming one cohesive memory event (Griffiths et al., 2019; Heusser et al., 2016; Karlsson et al., 2022; Lisman & Idiart, 1995; Lisman & Jensen, 2013; Ursino et al., 2023). Furthermore, it has been suggested that increased gamma

power during memory retrieval reflects hippocampal pattern completion leading to information reinstatement in the neocortex (Griffiths et al., 2019; Staresina et al., 2016). However, how this affects item memory, source memory, and memory confidence is not fully understood. The literature has suggested that hippocampal gamma is (indirectly) related to all three processes (Merkow et al., 2015), selectively related to source memory (Staresina et al., 2016), or that frontoparietal gamma is related to source memory (Burgess & Ali, 2002) and that posterior gamma is related to item memory (Gruber et al., 2008; Osipova et al., 2006). Most studies have investigated hippocampal gamma, and mainly its role in memory encoding. Therefore, it is currently unclear how neocortical gamma oscillations during retrieval are related to specific memory subprocesses.

The aim of the current exploratory study is to investigate how variability in memory accuracy (item, source) and memory confidence (high, low) relates to retrieval-related oscillatory power in the theta and gamma bands. Specifically, our participants performed a memory task where words were encoded in one of two conditions. During a subsequent memory recognition task, we probed their item memory accuracy, item memory confidence, source memory accuracy, and source memory confidence. Throughout the memory task, we recorded their brain activity via EEG. Linear mixed effect models were used to estimate the unique contribution of each of the behavioral measures to the trial-by-trial theta and gamma power during retrieval. Retrieval-related theta has been linked to item and source memory accuracy, and item memory confidence. If theta has a substantial unique contribution to each of these processes, this would be reflected by all these predictors being significant in the model. As the literature on the role of neocortical gamma oscillations is variable, it may be the case that retrieval-related gamma is related to only a subset of these behavioral outcomes. Not controlling the intercorrelations between measures could be a reason for mixed findings in the literature. Nonetheless, results from this study will inform us on the relative contribution of various memory subprocesses to the variability in theta and gamma oscillations.

## 2 | METHODS

### 2.1 | Participants

Fifty-four healthy adult right-handed volunteers (32 females, 22 males) with a mean age of 20 ( $SD = 1.55$ ) were included in this study. Data analyzed here were part of a larger noninvasive brain stimulation (NIBS) study, which included four sessions. Only the data from the first session are used here, where the participants did not receive any

NIBS. Four participants were replaced to maintain our intended sample size of 54, due to not adhering to task instructions ( $N=2$ ) and failure to complete all experimental sessions ( $N=2$ ). All had normal or corrected-to-normal vision, were fluent English speakers, right-handed, and free from self-reported neurological or psychiatric conditions. Main exclusion criteria were skin disease, metal in their cranium, epilepsy or a family history of epilepsy, history of other neurological conditions or psychiatric disease, heart disease, use of psychoactive medication or substances, and pregnancy. The study was approved by the institutional review board of Bowdoin College, Brunswick, USA, and carried out in accordance with the standards set by the Declaration of Helsinki.

## 2.2 | Stimuli

Stimuli were presented on a personal computer screen with a 21-inch monitor. Stimulus presentation and recording of responses were attained using E-Prime 2.0 software (Psychology Software Tools, Pittsburgh, PA). The stimulus material consisted of 400 words per session, varying per participant, randomly chosen from a pool of 1778 words, selected from the MRC Psycholinguistic Database ([http://websites.psychology.uwa.edu.au/school/MRCDatabase/](http://websites.psychology.uwa.edu.au/school/MRCDatabase/uwa_mrc.htm)

[uwa\\_mrc.htm](http://websites.psychology.uwa.edu.au/school/MRCDatabase/uwa_mrc.htm)). All words in this database are scored on word frequency, familiarity, and concreteness, which combined leads to an “imageability” rating between 100 and 700 (Coltheart, 1981). We only included nouns and adjectives that had an imageability rating of  $>300$ .

## 2.3 | Procedure

All participants received written and oral information prior to participation but remained naive regarding the aim of the study. Each volunteer provided written informed consent at the beginning of the first session.

In the intentional encoding phase of the memory task, trials began with the presentation of the response options on the bottom of the screen for 80–120 ms (jittered; see Figure 1). Throughout the trial, these response options remained on the screen. Next, the task cue (Place or Pleasant) was presented in the middle of the screen in yellow font for 500 ms, followed by a blank mask for 200 ms, and the presentation of the to-be-encoded capitalized word for 500 ms. The cue informed the participants on the encoding task in the current trial. When the cue “Place” was presented, participants had to conjure up an image of a scene of a spatial environment that relates to the word that was presented right after. For

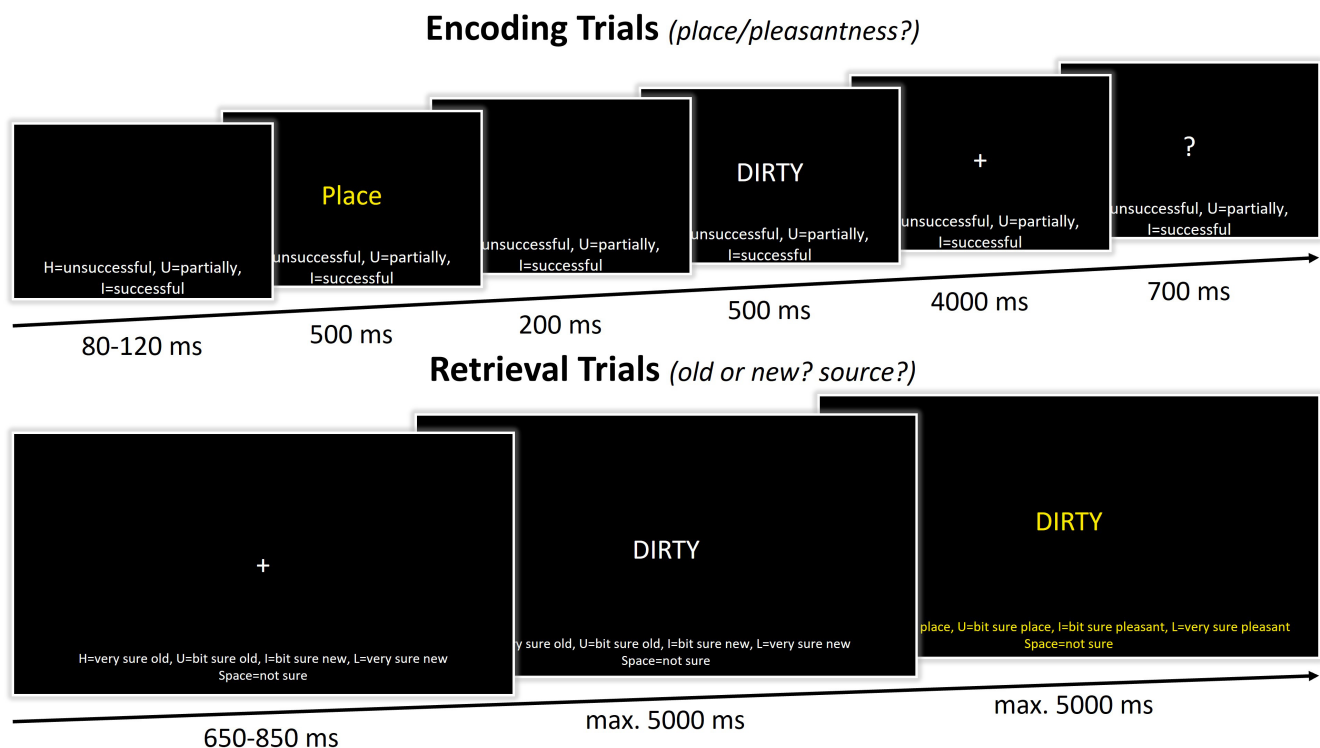


**FIGURE 1** Schematic overview of the memory task. In the encoding phase, participants either had to imagine a spatial scene (place task) or rate the pleasantness (pleasantness task) of the presented word. They indicated how successful they were in completing this encoding task. In the retrieval phase, participants first made an old/new response. In the case of an “old” response, participants were asked to indicate what encoding task was performed when first encountering that word.



example, for the word “dirty”, they could imagine a dirty scene or place, such as imagining a scene of a garbage dump or a messy room. When the cue “Pleasant” was presented, participants had to pay attention to the meaning of the word that was presented right after and evaluate how pleasant it is. For example, for the word “dirty”, they could imagine that it is “unpleasant”. Following the word offset, participants had 4 s to perform the encoding task while a fixation cross was presented on screen. Thereafter, a question mark replaced the fixation cross, and they had 700 ms to indicate how successful they were at completing the encoding task by responding on a keyboard with their dominant, right hand: “H” = unsuccessful, “U” = partially successful, “I” = successful. In total, there were 200 trials randomly intermixed: 100 words encoded during the place task and 100 words encoded during the pleasantness task.

After the encoding task, participants completed a math task to diminish any rehearsal and recency effect. In this task, mathematical equations (e.g.,  $56 + (5 + 5) \times 2 - 30$ ) were presented on the computer screen for 15 min. Participants were informed that this task was a distraction task, that they should not be nervous about it, and just try their best. The math task was self-paced, and participants could alter their answer prior to responding. Responses were attained using the numbers on the keyboard.

In the retrieval phase, participants performed a recognition task, including the 200 “old” words that were presented during encoding and 200 “new” words (see Figure 1). Like the encoding trials, the response options were presented on the bottom of the screen throughout the trial. The retrieval trials started with a 650- to 850-ms (jittered) presentation of a fixation cross. This was followed by a centrally presented capitalized word. Participants were instructed to indicate whether they thought the word was “old” or “new”, considering the confidence they had in their decision, on a 5-point scale. Responses were given on a keyboard with their dominant, right hand: “H” = very sure old, “U” = bit sure old, “space bar” = not sure, “I” = bit sure new, “L” = very sure new. Participants had 5 s to submit their response and their response would immediately advance the trial. However, to ensure a sufficient time frame for EEG analyses, within the first 800 ms of word presentation, entering a response would not advance the trial immediately. When their response was “not sure”, “bit sure new”, or “very sure new” the next trial started after their “old/new” decision was finalized. When their response was “bit sure old” or “very sure old,” a new screen was presented, and participants could indicate the encoding source of the word. On this screen, the source response options were presented: “H” = very sure pleasant, “U” = bit sure pleasant, “space bar” = not sure, “I” = bit sure place, “L” = very sure place. To make it more

salient to the participants that a source decision was now required, both the word in the center of the screen and the response options on the bottom were presented in a yellow font. Participants had 5 s to indicate their response on the keyboard, after which the next trial began.

To familiarize participants with the memory task, 15 practice trials preceded both the encoding and retrieval phases of the experiment. Stimuli used during the practice trials were not used in the experimental trials. Following every 100 experimental trials, there was a short break of a minimum of 30 s. Participants then had 30 s to indicate that they were ready to continue.

## 2.4 | EEG recording and analyses

EEG was recorded throughout the experimental session. EEG signals were recorded and amplified with an actiCHamp system (Brain Products, Munich, Germany) from 64 channels. Amplified analog voltages (0.1–100 Hz band-pass) were digitized at 10 kHz.

EEG preprocessing and analyses were performed with the use of MATLAB (v2022b, MathWorks Inc., Natick MA) in combination with the FieldTrip toolbox (Oostenveld et al., 2011) and the EEGLAB toolbox (Delorme & Makeig, 2004). Raw signals were downsampled to 1000 Hz and re-referenced to an average reference. The data were high-pass filtered at 0.1 Hz, low-pass filtered at 58 Hz, and an additional band-pass filter was used to remove additional line noise at 60 Hz. Subsequently, the retrieval data were epoched into stimulus-locked time windows. The minimum stimulus presentation duration during retrieval was 800 ms. However, since retrieval was self-paced, stimulus presentation duration varied. For this reason, epochs started 500 ms before stimulus onset and ended either 505 ms before the onset of the following stimulus or after 2000 ms. This resulted in the shortest retrieval epoch being –500 to 1045 ms, and the mean epoch length being –500 to 1810 ms. Epochs with transient muscle or electrode artifacts were rejected based on visual inspection. Additional artifacts were removed using independent component analysis (ICA) in combination with EEGLAB’s ICALabel (Pion-Tonachini et al., 2019). Components classified as muscle artifacts ( $p > .9$ ), eye artifacts ( $p > .8$ ), heart artifacts ( $p > .8$ ), and channel noise artifacts ( $p > .9$ ) were removed from the data. A final artifact check was done after ICA by manual inspection.

Spectral power for the lower frequencies was extracted using Fourier analysis with a 500-ms sliding time window and the application of a Hanning taper. Frequencies that were assessed ranged from 1 to 29 Hz in 1 Hz steps. Spectral power for the higher frequencies was extracted using Fourier analysis with a sliding time window of



10 cycles and a factor 0.2 smoothing per frequency, through the application of multitapers (3 Discrete Prolate Spheroidal Sequences [DPSS] tapers). Prior to spectral analysis, all data were zero padded to a total length of 5s. To prepare the data for further statistical analysis, for each trial, spectral data were averaged over the theta band (3–7 Hz) and gamma band (30–50 Hz), a 300–800 ms time window, and frontal (F1, F2, F3, F4, F5, F6, Fz) and parietal regions (P1, P2, P3, P4, P5, P6, Pz), based on previous EEG studies (Babiloni et al., 2004; Burgess & Ali, 2002; Gruber et al., 2008; Wynn et al., 2019, 2020). This gave us four variables: “Frontal Theta”, “Parietal Theta”, “Frontal Gamma”, and “Parietal Gamma”, which were used in further trial-by-trial analyses.

## 2.5 | Statistical analyses

All statistical analyses were performed in RStudio (RStudio version 2023.06.2, R version 4.2.0; R Core Team, 2021). For the behavioral analysis, hit rate, false alarm rate,  $d'$ , and high-confidence rate were calculated as follows:

$$\text{Item hit rate} = \frac{\text{hits}}{(\text{hits} + \text{misses})}$$

$$\text{Item false alarm rate} = \frac{\text{false alarms}}{(\text{false alarms} + \text{correct rejections})}$$

$$\text{Source hit rate} = \frac{\text{place hit}}{(\text{place hits} + \text{place misses})}$$

$$\text{Source false alarm rate} = \frac{\text{pleasantness misses}}{(\text{pleasantness hits} + \text{pleasantness misses})}$$

$$d' = z(\text{hit rate}) - z(\text{false alarm rate})$$

$$\text{High – confidence rate} = \frac{\text{high – confidence responses}}{\text{all responses}}$$

For these analyses, two-sided pairwise  $t$  tests were performed with an alpha of .05. Cohen's  $d$  was used as an effect size of the  $t$  tests.

For all trial-based oscillatory analyses, each trial was coded based on memory status (“old” or “new”) and memory accuracy (“correct” or “incorrect”), the combination of these two would make up the following memory categories: hits (“old” and “correct”), misses (“old” and “incorrect”), correct rejections (“new” and “correct”), and false alarms (“new” and “incorrect”). Due to the low number of “a bit sure” and “not sure” responses, these two responses were combined into one “low-confidence” level. Therefore, trial-based memory confidence on every trial was recoded

into “low” and “high” confidence. Outlier correction was performed on the trial-by-trial EEG data, with a cut-off of three standard deviations above or below the mean. For these analyses, linear mixed effects models were used to predict spectral power in the gamma and theta frequency bands from the behavioral responses from each individual trial (lme4 package [v. 1.1.29]; Bates et al., 2015). A mixed effect model was deemed most appropriate as it can account for within- and between-subject variability, through employing by-participant varying intercepts. Specifically, the following models were used in the analyses:

Item memory:

$$\text{model} < - \text{lmer}(\text{Oscillatory power} \sim \text{Brain region} \times (\text{Memory status} \times \text{Accuracy} + \text{Confidence}) + (1 \mid \text{Participant}))$$

Source memory:

$$\text{model} < - \text{lmer}(\text{Oscillatory power} \sim \text{Brain region} \times (\text{Accuracy} + \text{Confidence}) + (1 \mid \text{Participant}))$$

The fixed effects were Brain Region (“frontal”, “parietal”), Memory Status (“old”, “new”), Accuracy (“correct”, “incorrect”), and Confidence (“high”, “low”). As we were interested in two specific brain regions, we let Brain Region interact with the behavioral responses. Given that in item memory, we were interested in specific combinations of Memory Status and Accuracy, we also let those predictors interact. The combinations of interest in this study were old and correct (“hits”), new and correct (“correct rejections”), old and incorrect (“misses”), and new and incorrect (“false alarms”). In addition, we had by-participant varying intercepts, to consider individual differences. By-participant varying slopes were not included in these models as no large interindividual variability on specific fixed effects were anticipated. Therefore, to avoid overfitting, the less complex models with only random intercepts were selected. All categorical fixed effects were sum coded, and the linear outcome measure was standardized. These models were run separately for theta and gamma power, leading to four models used in total. Significance of the model outputs were generated by the lmerTest package (v. 3.1.3; Kuznetsova et al., 2017), which applies the Satterthwaite method for estimating degrees of freedom, with an alpha level of .05. In the case of a significant interaction, pairwise comparisons on the estimated marginal means were used to further investigate this. These comparisons were restricted to the following comparisons: hits versus correct rejections, hits versus misses, correct rejections versus false alarms, and high confidence versus low confidence. The first three were used to inform us on the effects of accuracy while controlling for confidence, whereas the last one was used to look at the effect of confidence while controlling for accuracy. The

variance inflation factor (VIF) for our variables of interest, Accuracy and Confidence, did not exceed a value of 2.54. This did not create any multicollinearity concern.

### 3 | RESULTS

#### 3.1 | Behavioral results

During encoding, participants successfully thought of either a place or the pleasantness regarding the presented word. The average imagining success was 87.37% ( $SD=8.40$ ), with no significant difference between the Pleasantness ( $M=87.35\%$ ,  $SD=10.07$ ) and Place ( $M=87.15\%$ ,  $SD=8.96$ ) conditions ( $t(53)=0.18$ ,  $p=.86$ ,  $d=.022$ ). After the fixed 4 s time window, their average imagining reaction time (RT) was 378 ms ( $SD=47$ ), with a significantly faster response in the Pleasantness ( $M=373$ ,  $SD=47$ ) than Place ( $M=383$ ,  $SD=48$ ) condition ( $t(53)=-3.75$ ,  $p<.001$ ,  $d=-.22$ ).

On average, participants went through 49 ( $SD=20.29$ ) math equations with an average response time of 19 s ( $SD=8.05$ ) and an accuracy of 77% ( $SD=14$ ). Given their performance, we deem it unlikely that participants were actively rehearsing items during the 20 min break between encoding and retrieval.

For the full description of the retrieval behavioral measures, see Table 1. The average item memory performance, as quantified by  $d'$ , was 2.31 ( $SD=0.59$ ) and the average RT, in ms, for the old/new judgment was 1642 ( $SD=309$ ). RTs showed a significant difference between the correct and incorrect old/new responses ( $t(53)=-12.06$ ,  $p<.001$ ,  $d=-.94$ ). The average source memory performance, as quantified by  $d'$ , was 1.64 ( $SD=0.73$ ) and the average RT for the source judgment was 1273 ( $SD=447$ ). RTs showed

a significant difference between correct and incorrect source responses ( $t(53)=-3.09$ ,  $p=.003$ ,  $d=-.33$ ). The results indicated that overall the Pleasantness and Place conditions were not significantly different, therefore they were combined in further analyses (see Table 1).

#### 3.2 | Oscillatory results

When investigating how elements of item memory predict theta power, the model showed that there was a significant three-way Brain region  $\times$  Memory status  $\times$  Accuracy interaction and a significant two-way Brain region  $\times$  Confidence interaction (see Figure 2 and Table 2). Post hoc tests (see Table 3) on the estimated marginal means revealed that predicted theta power was higher for hits, as compared to correct rejections and misses, in the frontal and parietal regions. In addition, theta power was significantly higher in high-confidence responses, as compared to low-confidence responses, in frontal and parietal regions. This indicates that theta oscillations play a role in both item memory accuracy and item memory confidence.

Regarding the relationship between theta power and source memory, the model showed that there was a marginal Brain region  $\times$  Accuracy interaction, and a significant main effect of Confidence (see Figure 3 and Table 4). Predicted theta was higher for high-confidence source decisions ( $M=0.15$ ,  $SE=0.096$ ), as compared to low-confidence source decisions ( $M=0.069$ ,  $SE=0.096$ ). This indicates that regarding source memory, there is evidence for the involvement of theta in memory confidence.

The model looking at the relationship between item memory and gamma power showed that there was a significant Brain region  $\times$  Accuracy interaction (see Figure 4 and Table 5). Post hoc tests (see Table 6) on the estimated

**TABLE 1** Mean values of behavioral performance during memory retrieval, with the standard deviation in brackets.

	Item memory			Source memory		
	All	Place	Pleasantness	All	Place	Pleasantness
Hit rate	.77 (.09)	.76 (.10)	.78 (.10)	.72 (.15)	–	–
False alarm rate	.08 (.07)	–	–	.18 (.11)	–	–
$d'$	2.31 (.59)	2.29 (.59)	2.34 (.63)	1.64 (.73)	–	–
HC responses (%)	.61 (.21)	–	–	.54 (.22)	–	–
HC hits (%)	.83 (.13)	.83 (.13)	.83 (.14)	.68 (.22)	.72 (.22)	.63 (.24)*
HC correct rejections (%)	.52 (.30)	–	–	–	–	–
RT all trials (in ms)	1642 (309)	1663 (333)	1664 (320)	1273 (447)	1256 (452)	1284 (472)
RT correct trials (in ms)	1587 (292)	1646 (342)	1626 (323)	1258 (503)	1242 (516)	1292 (535)
RT incorrect trials (in ms)	1911 (392)	1779 (431)	1845 (424)	1423 (504)	1451 (559)	1412 (506)

Note: Significant differences between Place and Pleasantness conditions are indicated in the table.

Abbreviations: HC, high confidence, RT, reaction time.

\* $p<.05$ .

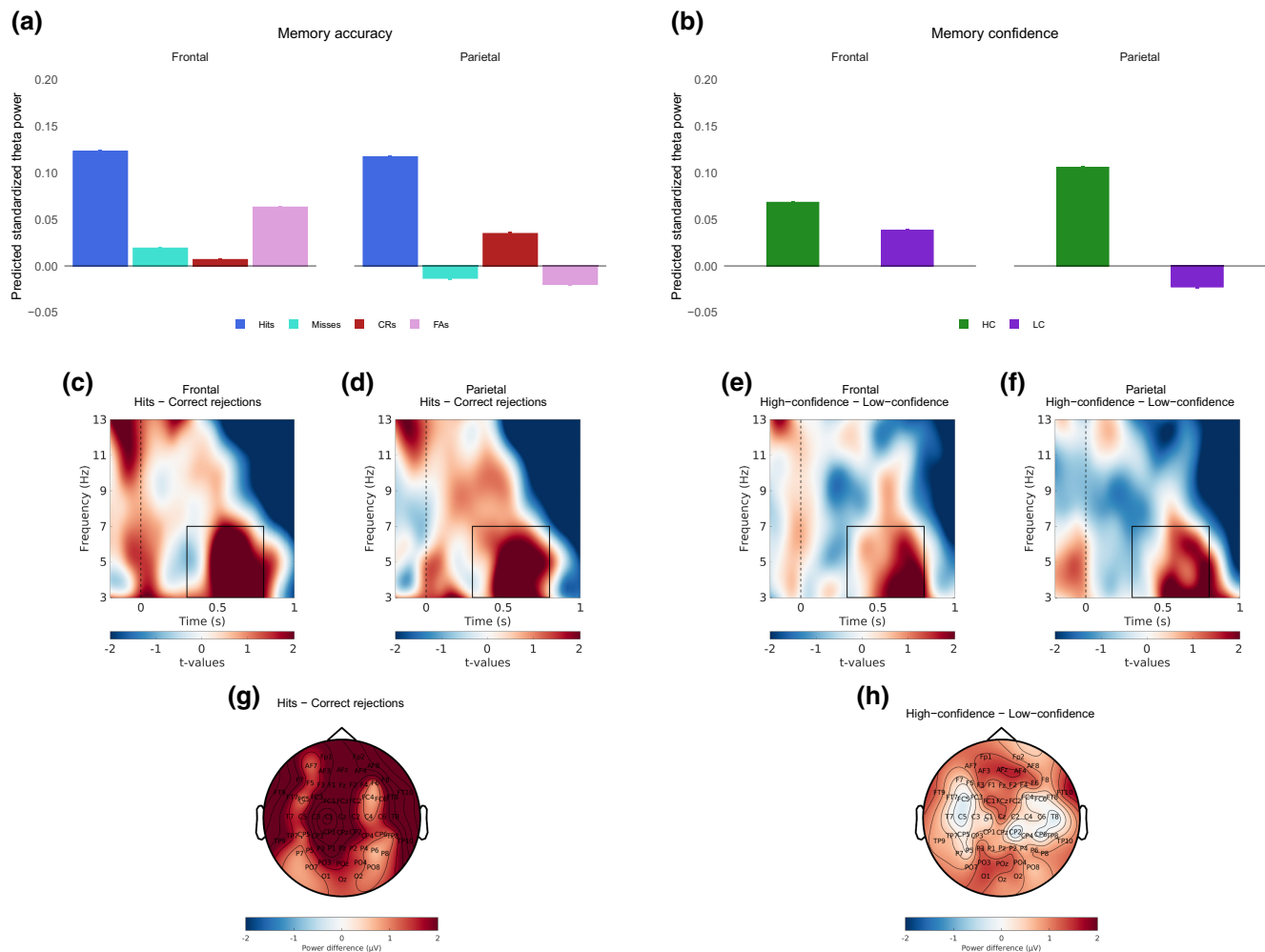


**FIGURE 2** The relationship between theta power and item memory. (a) Predicted standardized power obtained from the linear mixed effect model for the memory accuracy conditions (hits, misses, correct rejections, false alarms), for frontal and parietal regions. The values shown reflect predicted theta while controlling for the other predictors in the model, like memory confidence. (b) Predicted standardized power obtained from the linear mixed effect model for the memory confidence conditions (high-confidence, low-confidence), for frontal and parietal regions. The values shown reflect predicted theta while controlling for the other predictors in the model, like memory accuracy. The frequency and time window used for the models is indicated in the lower plots by a rectangle. (c) The  $t$  values of the difference in power between hits and correct rejections for the frontal EEG channels. (d) The  $t$  values of the difference in power between hits and correct rejections for the parietal EEG channels. (e) The  $t$  values of the difference in power between high and low confidence for the frontal EEG channels. (f) The  $t$  values of the difference in power between high and low confidence for the parietal EEG channels. (g) The topographical representation showing the  $t$  values of the difference in power between hits and correct rejections. (h) The topographical representation showing the  $t$  values of the difference in power between high and low confidence. Note that the  $t$  values here are only for illustration purposes and are separate from the model-based analysis discussed in the article.

marginal means revealed that the predicted frontal gamma power was significantly higher for false alarms, as compared to correct rejections. The opposite pattern was found for parietal gamma power. In addition, parietal gamma power was increased for hits, as compared to misses. This indicates that gamma oscillations not only play a role in item memory accuracy, specifically novelty processing, but also in memory retrieval in the parietal region.

Regarding the relationship between gamma power and source memory, the model showed that there was

a significant main effect of Accuracy and a significant Brain region  $\times$  Confidence interaction (see Figure 5 and Table 7). Predicted gamma was lower for correct source decisions ( $M=0.074$ ,  $SE=0.11$ ) than incorrect source decisions ( $M=0.10$ ,  $SE=0.11$ ). Post hoc tests (see Table 8) on the estimated marginal means revealed that in the frontal region, predicted gamma power was significantly higher for low-confidence responses, as compared to high-confidence responses. The opposite pattern was found in the parietal region, there predicted gamma power was significantly higher for high-confidence responses, as

	Estimate	SE	df	t	p
Intercept	0.011	0.093	56	0.114	.909
Brain region	0.054	0.015	33,445	3.547	.000*
Memory status	−0.025	0.020	33,450	−1.264	.206
Accuracy	−0.017	0.017	33,453	−1.007	.314
Confidence	0.049	0.010	33,474	4.764	.000*
Memory status × Accuracy	0.110	0.022	33,452	5.048	.000*
Brain region × Memory status	−0.019	0.019	33,445	−0.977	.329
Brain region × Accuracy	−0.038	0.016	33,445	−2.288	.022*
Brain region × Confidence	−0.054	0.009	33,445	−5.856	.000*
Brain region × Memory status × Accuracy	0.051	0.021	33,445	2.407	.016*

Note: Significant coefficients are indicated in the table.

\* $p < .05$ .

**TABLE 2** Theta—item memory: Model.

**TABLE 3** Theta—item memory: Pairwise comparisons.

Brain region	Comparison	Estimate	SE	df	Z ratio	p	Cohen's d
Frontal	Hit - CR	0.116	0.013	Inf	9.060	.000*	0.156
	Hit - Miss	0.104	0.019	Inf	5.348	.000*	0.140
	CR - FA	−0.056	0.023	Inf	−2.415	.074 <sup>+</sup>	−0.076
	HC - LC	0.030	0.013	Inf	2.384	.017*	0.040
Parietal	Hit - CR	0.083	0.013	Inf	6.423	.000*	0.111
	Hit - Miss	0.130	0.019	Inf	6.690	.000*	0.175
	CR - FA	0.054	0.023	Inf	2.330	.091 <sup>+</sup>	0.073
	HC - LC	0.128	0.013	Inf	10.221	.000*	0.172

Note: Significant differences are indicated in the table.

\* $p < .05$ .

<sup>+</sup> $p < .1$ .

compared to low-confidence responses. This indicates that gamma plays a role in both source memory accuracy and confidence.

## 4 | DISCUSSION

This EEG study explored how variability in objective and subjective item and source memory influences theta and gamma oscillations. By utilizing a source memory task that incorporates confidence ratings, we were able to investigate item and source memory, and their respective accuracy and confidence levels. A model-based approach was used to disentangle the unique contributions of each of these behavioral measures to the trial-by-trial theta and gamma power during retrieval.

When we focus on theta oscillations, our results show that most of the behavioral measures we investigated influenced theta power measured during retrieval

(see Table 9), which is in line with previous literature (Addante et al., 2011; Duzel et al., 2005; Gruber et al., 2008; Wynn et al., 2019, 2020). These studies showed greater theta power for hits than correct rejection and misses, and greater theta power for high-confidence than low-confidence responses. Here, we replicate these findings and show that these findings remain unchanged when other correlated variables are kept constant. Specifically, when controlling for memory confidence, we found memory accuracy effects, and when controlling for memory accuracy, we found memory confidence effects. The association between item confidence and theta was found in both the frontal and parietal region. This is consistent with previous studies which have linked frontal and parietal theta to memory confidence (Wynn et al., 2019, 2020). However, it is of note that we did not find a significant relationship between theta power and source memory accuracy, given the literature showing this relation (Addante et al., 2011;



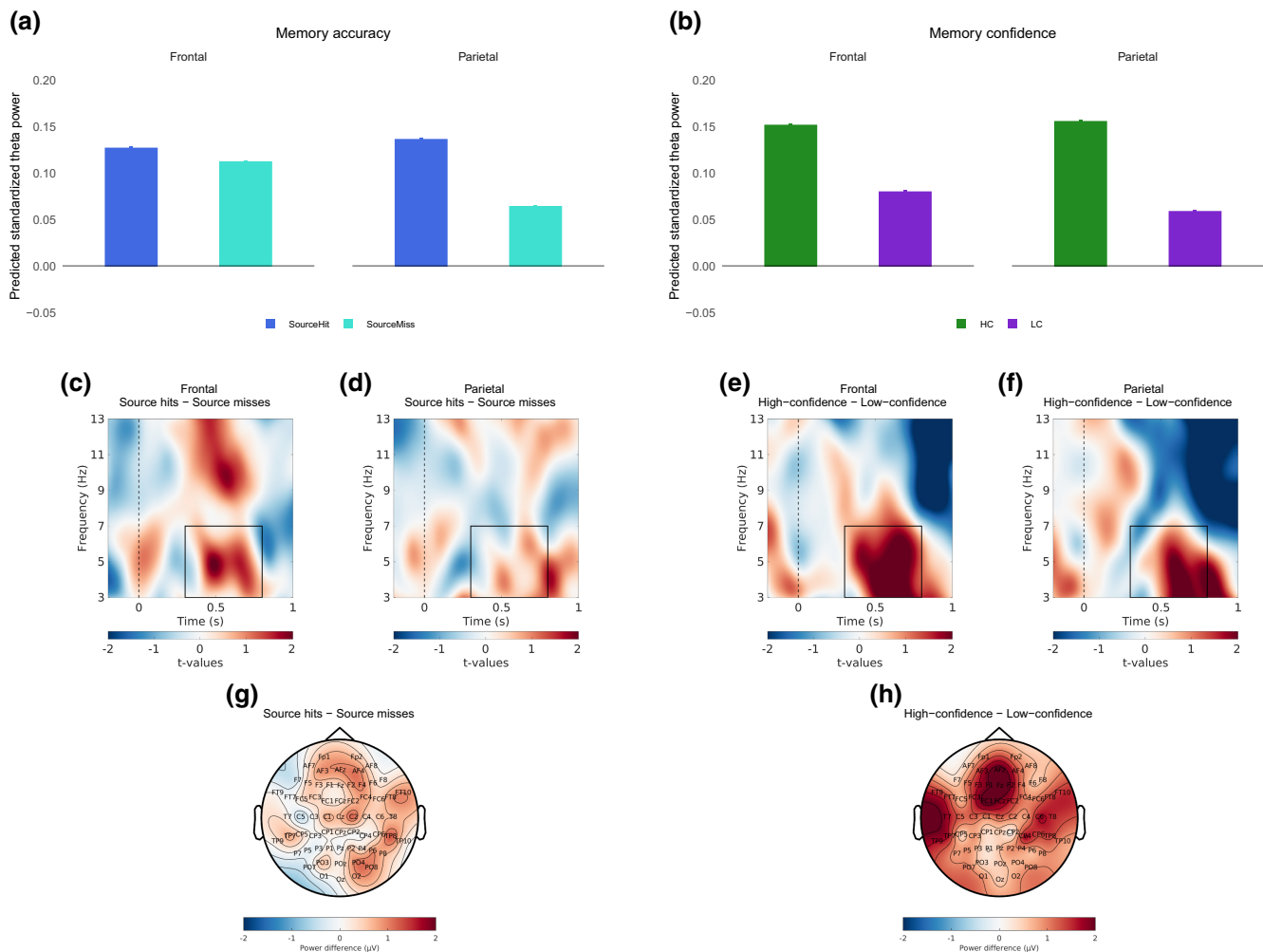


**FIGURE 3** The relationship between theta power and source memory. (a) Predicted standardized power obtained from the linear mixed effect model for the memory accuracy conditions (source hits, source misses), for frontal and parietal regions. The values shown reflect predicted theta while controlling for the other predictors in the model, like memory confidence. (b) Predicted standardized power obtained from the linear mixed effect model for the memory confidence conditions (high-confidence, low-confidence), for frontal and parietal regions. The values shown reflect predicted theta while controlling for the other predictors in the model, like memory accuracy. The frequency and time window used for the models is indicated in the lower plots by a rectangle. (c) The  $t$  values of the difference in power between source hits and source misses for the frontal EEG channels. (d) The  $t$  values of the difference in power between source hits and source misses for the parietal EEG channels. (e) The  $t$  values of the difference in power between high and low confidence for the frontal EEG channels. (f) The  $t$  values of the difference in power between high and low confidence for the parietal EEG channels. (g) The topographical representation showing the  $t$  values of the difference in power between source hits and source misses. (h) The topographical representation showing the  $t$  values of the difference in power between high and low confidence. Note that the  $t$  values here are only for illustration purposes and are separate from the model-based analysis discussed in the article.

**TABLE 4** Theta—source memory: Model.

	Estimate	SE	df	$t$	$p$
Intercept	0.063	0.096	55	0.657	.514
Brain region	0.025	0.014	12,705	1.809	.070 <sup>+</sup>
Accuracy	0.011	0.017	12,714	0.635	.526
Confidence	0.081	0.017	12,731	4.885	.000*
Brain region × Accuracy	−0.027	0.016	12,705	−1.656	.098 <sup>+</sup>
Brain region × Confidence	−0.004	0.015	12,705	−0.239	.811

Note: Significant coefficients are indicated in the table.

\* $p < .05$ .

<sup>+</sup> $p < .1$ .

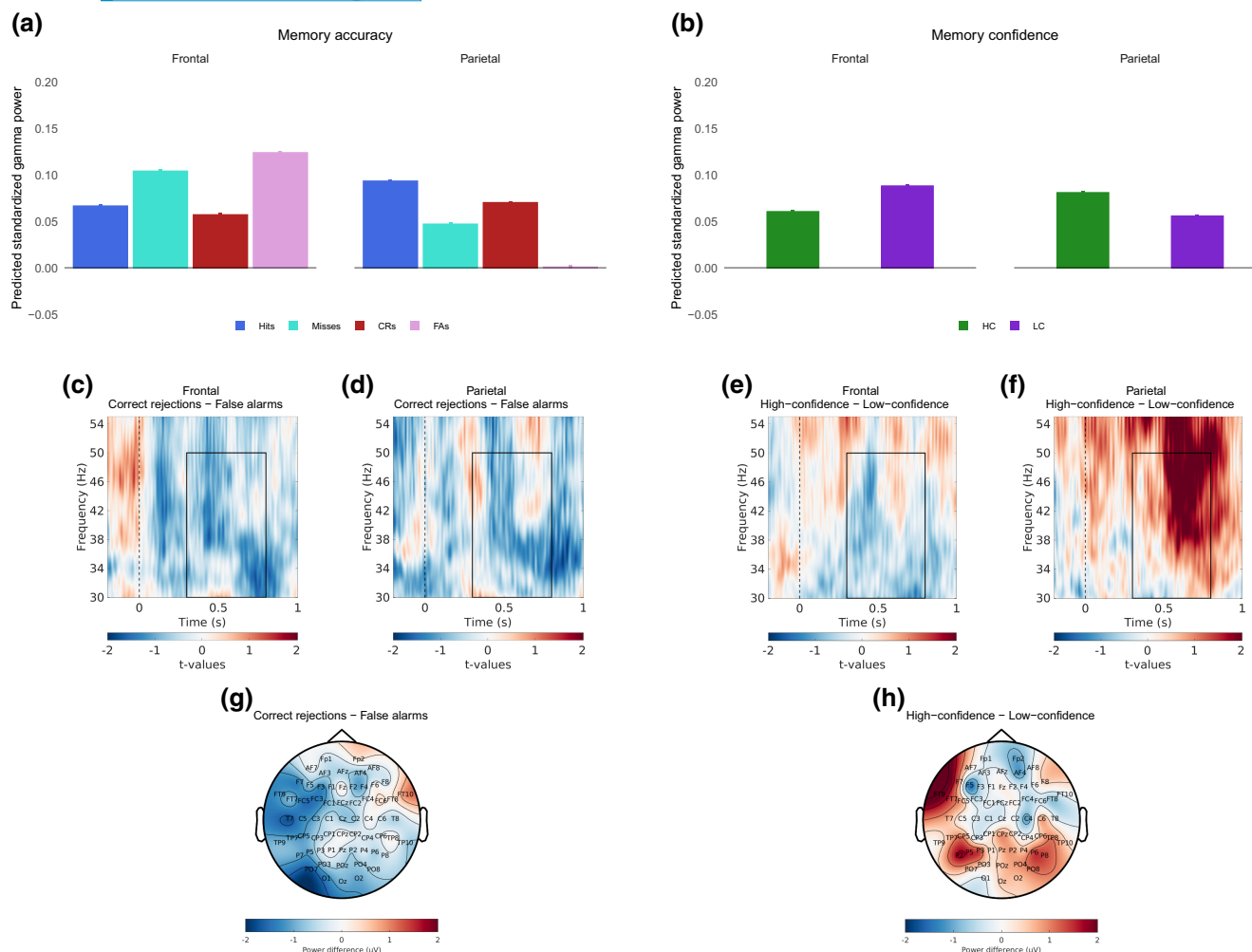


**FIGURE 4** The relationship between gamma power and item memory. (a) Predicted standardized power obtained from the linear mixed effect model for the memory accuracy conditions (hits, misses, correct rejections, false alarms), for frontal and parietal regions. The values shown reflect predicted gamma while controlling for the other predictors in the model, like memory confidence. (b) Predicted standardized power obtained from the linear mixed effect model for the memory confidence conditions (high-confidence, low-confidence), for frontal and parietal regions. The values shown reflect predicted gamma while controlling for the other predictors in the model, like memory accuracy. The frequency and time window used for the models is indicated in the lower plots by a rectangle. (c) The  $t$  values of the difference in power between correct rejections and false alarms for the frontal EEG channels. (d) The  $t$  values of the difference in power between correct rejections and false alarms for the parietal EEG channels. (e) The  $t$  values of the difference in power between high and low confidence for the frontal EEG channels. (f) The  $t$  values of the difference in power between high and low confidence for the parietal EEG channels. (g) The topographical representation showing the  $t$  values of the difference in power between correct rejections and false alarms. (h) The topographical representation showing the  $t$  values of the difference in power between high and low confidence. Note that the  $t$  values here are only for illustration purposes and are separate from the model-based analysis discussed in the article.

Gruber et al., 2008; Guderian & Duzel, 2005; Herweg et al., 2016). In this study, the role of theta in source memory seemed to be specific to source memory confidence, a measure which is not often included in analyses. Our findings thus suggest that previous associations between theta power and source memory accuracy may have been mediated by a confidence effect.

The theta effects we found on memory accuracy seemed to be specific to retrieving information from memory, as compared to novelty detection. Given that

theta power differentiated between correct and incorrect responses for old items, but not new items. This seems to contradict previous literature reporting a link between evoked frontal theta and novelty processing (Wynn et al., 2019, 2020). However, these studies showed an interaction between the novelty effect and memory confidence, not a main effect. Here we did not investigate any interactions between memory accuracy and confidence since our main focus was disentangling the unique effects of behavioral measures. Furthermore,

**TABLE 5** Gamma—item memory: Model.

	Estimate	SE	df	t	p
Intercept	0.064	0.107	55	0.593	.555
Brain region	0.064	0.014	33,345	4.723	.000*
Memory status	0.014	0.018	33,348	0.793	.428
Accuracy	0.004	0.015	33,350	0.230	.818
Confidence	−0.007	0.009	33,364	−0.745	.456
Memory status × Accuracy	0.004	0.020	33,350	0.216	.829
Brain region × Memory status	−0.031	0.017	33,345	−1.805	.071 <sup>+</sup>
Brain region × Accuracy	−0.064	0.015	33,345	−4.272	.000*
Brain region × Confidence	−0.013	0.008	33,345	−1.604	.109
Brain region × Memory status × Accuracy	0.028	0.019	33,345	1.474	.141

Note: Significant coefficients are indicated in the table.

\* $p < .05$ .

<sup>+</sup> $p < .1$ .

**TABLE 6** Gamma—item memory: Pairwise comparisons.

Brain region	Comparison	Estimate	SE	df	Z ratio	p	Cohen's d
Frontal	Hit - CR	0.009	0.012	Inf	0.815	.848	0.014
	Hit - Miss	−0.038	0.018	Inf	−2.129	.144	−0.056
	CR - FA	−0.067	0.021	Inf	−3.16	.009*	−0.099
Parietal	Hit - CR	0.023	0.012	Inf	1.998	.189	0.034
	Hit - Miss	0.046	0.018	Inf	2.629	.043*	0.069
	CR - FA	0.069	0.021	Inf	3.281	.006*	0.103

Note: Significant differences are indicated in the table.

\* $p < .05$ .

previous findings were specific to evoked theta, while here no distinction was made between evoked and induced theta. This could indicate that novelty effects may be specific to time- and phase-locked theta oscillations. Another explanation for these findings is that the main role of theta power pertains to memory confidence, which mediates subsequent novelty decisions in a similar way it can mediate source memory decisions. Overall, our theta results are in concordance with previous literature showing a link between theta power and both memory accuracy and confidence. This study additionally provides evidence for independent relations between these memory measures and retrieval-related theta oscillations. Moreover, it supports the hypothesis that theta power plays a significant role in memory-related decision making, given the positive relationship with memory confidence.

Our findings also add evidence for a link between retrieval-related processes and neocortical gamma oscillations (see Table 9). Previous studies have linked gamma oscillations to item and source memory accuracy (Burgess & Ali, 2002; Gruber et al., 2008) and decision-making

processes (Castelhano et al., 2014; Polanía et al., 2014). Our results are in accordance with this by showing a link between gamma and both memory accuracy and source memory confidence. The latter supports the involvement in decision-making processes regarding source memories. Interestingly, the link between gamma oscillations and memory seems to differ between frontal and parietal regions. In the frontal region, there were negative relationships, while there were mainly positive ones in the parietal region. Regarding item memory, we found a decrease in frontal gamma and an increase in parietal gamma for correct rejections, as compared to false alarms. A similar pattern of results is reported by Summerfield and Mangels (2005) who investigated gamma power during the performance of a Deese–Roediger–McDermott (DRM) task. They additionally conclude that activity in the gamma band facilitates frontoparietal synchronization needed for memory recognition.

From our findings, it appears that frontal gamma activity is higher when participants are incorrect or unsure about their decision. These behavioral outcomes are expected in situations where more cognitive control is

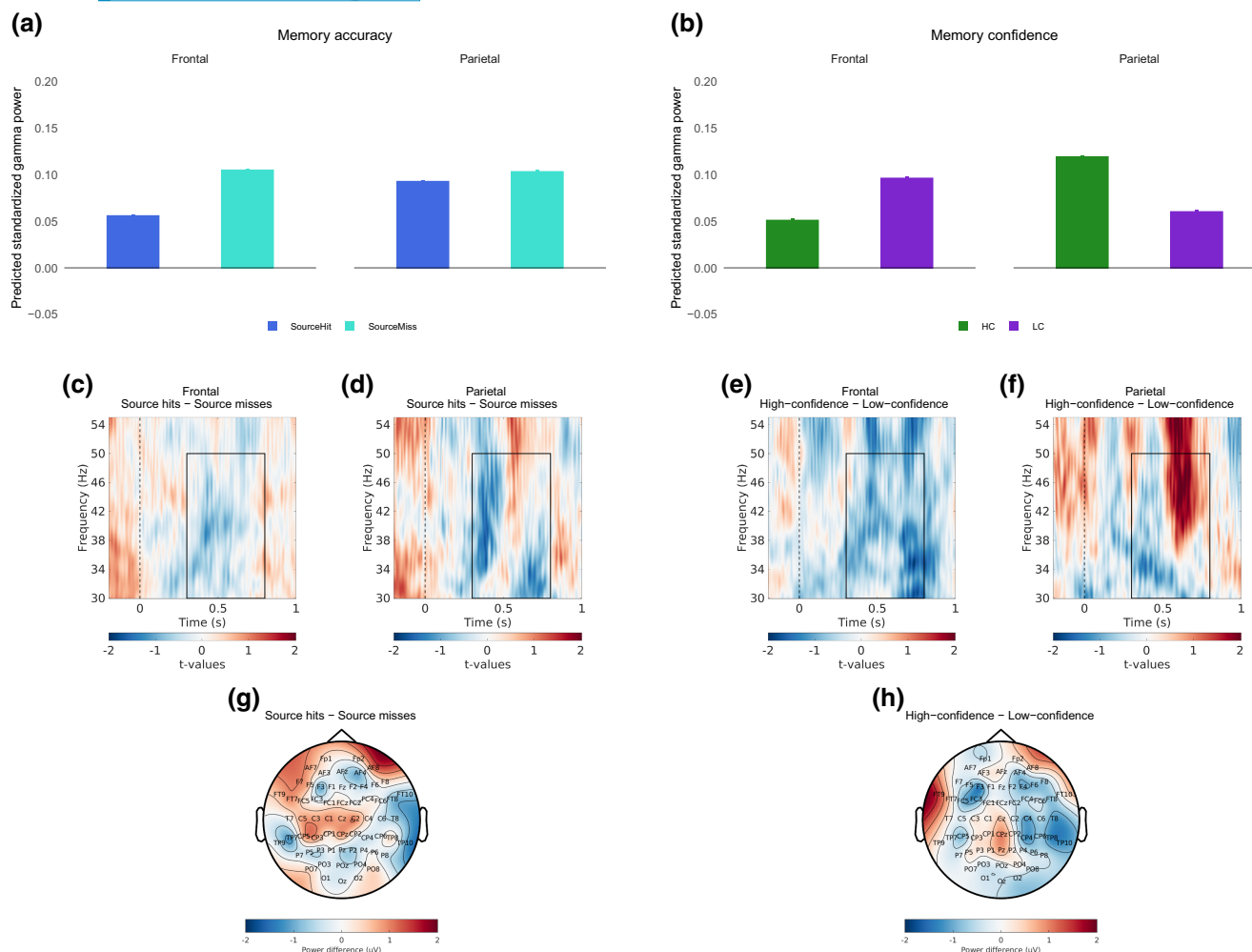


**FIGURE 5** The relationship between gamma power and source memory. (a) Predicted standardized power obtained from the linear mixed effect model for the memory accuracy conditions (source hits, source misses), for frontal and parietal regions. The values shown reflect predicted gamma while controlling for the other predictors in the model, like memory confidence. (b) Predicted standardized power obtained from the linear mixed effect model for the memory confidence conditions (high-confidence, low-confidence), for frontal and parietal regions. The values shown reflect predicted gamma while controlling for the other predictors in the model, like memory accuracy. The frequency and time window used for the models is indicated in the lower plots by a rectangle. (c) The  $t$  values of the difference in power between source hits and source misses for the frontal EEG channels. (d) The  $t$  values of the difference in power between source hits and source misses for the parietal EEG channels. (e) The  $t$  values of the difference in power between high and low confidence for the frontal EEG channels. (f) The  $t$  values of the difference in power between high and low confidence for the parietal EEG channels. (g) The topographical representation showing the  $t$  values of the difference in power between source hits and source misses. (h) The topographical representation showing the  $t$  values of the difference in power between high and low confidence. Note that the  $t$  values here are only for illustration purposes and are separate from the model-based analysis discussed in the article.

	Estimate	SE	df	$t$	$p$
Intercept	0.098	0.108	54	0.912	.366
Brain region	0.017	0.012	12,705	1.389	.165
Accuracy	−0.038	0.015	12,711	−2.498	.012*
Confidence	0.019	0.015	12,722	1.327	.185
Brain region × Accuracy	0.002	0.015	12,705	0.134	.894
Brain region × Confidence	−0.053	0.013	12,705	−4.015	.000*

Note: Significant coefficients are indicated in the table.

\* $p < .05$ .

**TABLE 7** Gamma—source memory: Model.



**TABLE 8** Gamma—source memory: Pairwise comparisons.

Brain region	Comparison	Estimate	SE	df	Z ratio	p	Cohen's d
Frontal	HC - LC	−0.045	0.018	Inf	−2.458	.014*	−0.067
Parietal	HC - LC	0.059	0.018	Inf	3.210	.001*	0.087

Note: Significant differences are indicated in the table.

\* $p < .05$ .

**TABLE 9** Summary of relationships between oscillatory power and behavioral measurements.

Oscillation	Brain region	Item memory		Source memory	
		Accuracy	Confidence	Accuracy	Confidence
Theta	Frontal	+	+		+
	Parietal	+	+		
Gamma	Frontal	−		−	−
	Parietal	+			+

Note: Significant positive relationships indicated with a “+” and significant negative ones with a “−”.

required as the retrieval process is more difficult. Previous literature has shown that frontal gamma oscillations are linked to top-down control in memory retrieval (Keizer et al., 2010) and that gamma oscillations support attentional control in the frontoparietal network (Helfrich & Knight, 2016). It therefore seems that our frontal gamma effects could reflect the way the PFC exerts cognitive control over memory processes during post-retrieval monitoring (Nyhus & Badre, 2015; Rugg, 2022). The frontal control mechanisms may mediate the attentional and evidence accumulation related processes in the parietal cortex (Cabeza et al., 2008; Zhang et al., 2022), especially when there is a high level of uncertainty. The increase in parietal power for item memory accuracy and source memory confidence would then reflect the attention to memory and/or the amount of accumulated evidence to make the memory decision. Overall, our results add to the sparse literature on the role of neocortical gamma and memory processing, by linking gamma power to memory-related frontoparietal communication.

It is important to mention that since our choices of time window, frequencies, and channels were set a priori based on previous literature (Babiloni et al., 2004; Burgess & Ali, 2002; Gruber et al., 2008; Wynn et al., 2019, 2020), it in some cases did not seem to align with where the effects appear strongest in our data. This can be seen as a limitation, given that our models could perhaps be improved by tweaking these parameters to match our actual data. However, if we had selected our data that went into the models based on visual inspection of the data or statistical tests, this would have biased our models and the associated statistical analyses. For this reason, we opted to select our data based on parameters from prior studies. As we have provided graphical representations of our data and

have made these data available, researchers can use this in their future choices regarding these parameters.

To summarize, we utilized a trial-by-trial model-based approach to uncover the unique relationships between behavioral memory measures and neuronal oscillations. Our results indicate that theta and gamma oscillations are linked to both memory accuracy and confidence. However, while theta oscillations seem to primarily play a role in memory-related confidence, gamma oscillations appear to reflect multiple memory processes, dependent on brain area.

## AUTHOR CONTRIBUTIONS

**Syanah C. Wynn:** Conceptualization; data curation; formal analysis; investigation; methodology; project administration; resources; supervision; visualization; writing – original draft; writing – review and editing. **Christopher D. Townsend:** Formal analysis; methodology; visualization; writing – review and editing. **Erika Nyhus:** Conceptualization; funding acquisition; project administration; resources; supervision; writing – review and editing.

## ACKNOWLEDGMENTS

This work was supported by the National Institutes of Health (NIH) grant R15MH114190. We thank Brandon Lee for his assistance in data collection.

## CONFLICT OF INTEREST STATEMENT

None.

## DATA AVAILABILITY STATEMENT

The data that support the findings of this study are openly available in OSF at DOI [10.17605/OSF.IO/](https://doi.org/10.17605/OSF.IO/)

RU9NQ and Github at <https://github.com/SyanahWynn/2024-EEGMEM>.

## ORCID

Syanah C. Wynn  <https://orcid.org/0000-0002-8002-9772>

Christopher D. Townsend  <https://orcid.org/0000-0003-4620-0924>

Erika Nyhus  <https://orcid.org/0000-0001-9601-2396>

## REFERENCES

- Addante, R. J., Watrous, A. J., Yonelinas, A. P., Ekstrom, A. D., & Ranganath, C. (2011). Prestimulus theta activity predicts correct source memory retrieval. *Proceedings of the National Academy of Sciences of the United States of America*, 108(26), 10702–10707. <https://doi.org/10.1073/pnas.1014528108>
- Babiloni, C., Babiloni, F., Carducci, F., Cappa, S., Cincotti, F., del Percio, C., Miniussi, C., Moretti, D. V., Pasqualetti, P., Rossi, S., Sosta, K., & Rossini, P. M. (2004). Human cortical EEG rhythms during long-term episodic memory task. A high-resolution EEG study of the HERA model. *NeuroImage*, 21(4), 1576–1584. <https://doi.org/10.1016/j.neuroimage.2003.11.023>
- Bates, D., Mächler, M., Bolker, B., & Walker, S. (2015). Fitting linear mixed-effects models using lme4. *Journal of Statistical Software*, 67(1), 1–48. <https://doi.org/10.18637/jss.v067.i01>
- Burgess, A. P., & Ali, L. (2002). Functional connectivity of gamma EEG activity is modulated at low frequency during conscious recollection. *International Journal of Psychophysiology*, 46(2), 91–100. [https://doi.org/10.1016/s0167-8760\(02\)00108-3](https://doi.org/10.1016/s0167-8760(02)00108-3)
- Cabeza, R., Ciaramelli, E., Olson, I. R., & Moscovitch, M. (2008). The parietal cortex and episodic memory: An attentional account. *Nature Reviews. Neuroscience*, 9(8), 613–625. <https://doi.org/10.1038/nrn2459>
- Castelhano, J., Duarte, I. C., Wibrál, M., Rodriguez, E., & Castelo-Branco, M. (2014). The dual facet of gamma oscillations: Separate visual and decision making circuits as revealed by simultaneous EEG/fMRI. *Human Brain Mapping*, 35(10), 5219–5235.
- Chrastil, E. R., Rice, C., Goncalves, M., Moore, K. N., Wynn, S. C., Stern, C. E., & Nyhus, E. (2022). Theta oscillations support active exploration in human spatial navigation. *NeuroImage*, 262, 119581. <https://doi.org/10.1016/j.neuroimage.2022.119581>
- Coltheart, M. (1981). The MRC psycholinguistic database. *The Quarterly Journal of Experimental Psychology A: Human Experimental Psychology*, 33A(4), 497–505. <https://doi.org/10.1080/14640748108400805>
- Delorme, A., & Makeig, S. (2004). EEGLAB: An open source toolbox for analysis of single-trial EEG dynamics including independent component analysis. *Journal of Neuroscience Methods*, 134(1), 9–21. <https://doi.org/10.1016/j.jneumeth.2003.10.009>
- Duzel, E., Habib, R., Rotte, M., Guderian, S., Tulving, E., & Heinze, H. J. (2003). Human hippocampal and parahippocampal activity during visual associative recognition memory for spatial and nonspatial stimulus configurations. *The Journal of Neuroscience*, 23(28), 9439–9444. <https://doi.org/10.1523/JNEUROSCI.23-28-09439.2003>
- Duzel, E., Neufang, M., & Heinze, H. J. (2005). The oscillatory dynamics of recognition memory and its relationship to event-related responses. *Cerebral Cortex*, 15(12), 1992–2002. <https://doi.org/10.1093/cercor/bhi074>
- Griffiths, B. J., & Jensen, O. (2023). Gamma oscillations and episodic memory. *Trends in Neurosciences*, 46, 832–846. <https://doi.org/10.1016/j.tins.2023.07.003>
- Griffiths, B. J., Martin-Buro, M. C., Staesina, B. P., & Hanslmayr, S. (2021). Disentangling neocortical alpha/beta and hippocampal theta/gamma oscillations in human episodic memory formation. *NeuroImage*, 242, 118454. <https://doi.org/10.1016/j.neuroimage.2021.118454>
- Griffiths, B. J., Parish, G., Roux, F., Michelmann, S., van der Plas, M., Kolibius, L. D., Chelvarajah, R., Rollings, D. T., Sawlani, V., Hamer, H., Gollwitzer, S., Kreiselmeier, G., Staesina, B., Wimber, M., & Hanslmayr, S. (2019). Directional coupling of slow and fast hippocampal gamma with neocortical alpha/beta oscillations in human episodic memory. *Proceedings of the National Academy of Sciences of the United States of America*, 116(43), 21834–21842. <https://doi.org/10.1073/pnas.1914180116>
- Gruber, T., Tsivilis, D., Giabbiconi, C. M., & Muller, M. M. (2008). Induced electroencephalogram oscillations during source memory: Familiarity is reflected in the gamma band, recollection in the theta band. *Journal of Cognitive Neuroscience*, 20(6), 1043–1053. <https://doi.org/10.1162/jocn.2008.20068>
- Guderian, S., & Duzel, E. (2005). Induced theta oscillations mediate large-scale synchrony with mediotemporal areas during recollection in humans. *Hippocampus*, 15(7), 901–912. <https://doi.org/10.1002/hipo.20125>
- Hanslmayr, S., Staesina, B. P., & Bowman, H. (2016). Oscillations and episodic memory: Addressing the synchronization/desynchronization conundrum. *Trends in Neurosciences*, 39(1), 16–25. <https://doi.org/10.1016/j.tins.2015.11.004>
- Helfrich, R. F., & Knight, R. T. (2016). Oscillatory dynamics of prefrontal cognitive control. *Trends in Cognitive Sciences*, 20(12), 916–930. <https://doi.org/10.1016/j.tics.2016.09.007>
- Herweg, N. A., Apitz, T., Leicht, G., Mulert, C., Fuentemilla, L., & Bunzeck, N. (2016). Theta-alpha oscillations bind the hippocampus, prefrontal cortex, and striatum during recollection: Evidence from simultaneous EEG-fMRI. *The Journal of Neuroscience*, 36(12), 3579–3587. <https://doi.org/10.1523/JNEUROSCI.3629-15.2016>
- Herweg, N. A., Solomon, E. A., & Kahana, M. J. (2020). Theta oscillations in human memory. *Trends in Cognitive Sciences*, 24(3), 208–227. <https://doi.org/10.1016/j.tics.2019.12.006>
- Heusser, A. C., Poeppel, D., Ezzyat, Y., & Davachi, L. (2016). Episodic sequence memory is supported by a theta-gamma phase code. *Nature Neuroscience*, 19(10), 1374–1380. <https://doi.org/10.1038/nn.4374>
- Jensen, O., Kaiser, J., & Lachaux, J. P. (2007). Human gamma-frequency oscillations associated with attention and memory. *Trends in Neurosciences*, 30(7), 317–324. <https://doi.org/10.1016/j.tins.2007.05.001>
- Karlsson, A. E., Lindenberger, U., & Sander, M. C. (2022). Out of rhythm: Compromised precision of theta-gamma coupling impairs associative memory in old age. *The Journal of Neuroscience*, 42(9), 1752–1764. <https://doi.org/10.1523/JNEUROSCI.1678-21.2021>
- Keizer, A. W., Verment, R. S., & Hommel, B. (2010). Enhancing cognitive control through neurofeedback: A role of gamma-band activity in managing episodic retrieval. *NeuroImage*, 49(4), 3404–3413. <https://doi.org/10.1016/j.neuroimage.2009.11.023>

- Kuznetsova, A., Brockhoff, P. B., & Christensen, R. H. (2017). lmerTest package: Tests in linear mixed effects models. *Journal of Statistical Software*, 82, 1–26.
- Lega, B., Burke, J., Jacobs, J., & Kahana, M. J. (2016). Slow-theta-to-gamma phase-amplitude coupling in human hippocampus supports the formation of new episodic memories. *Cerebral Cortex*, 26(1), 268–278. <https://doi.org/10.1093/cercor/bhu232>
- Lisman, J. E., & Idiart, M. A. (1995). Storage of 7 +/- 2 short-term memories in oscillatory subcycles. *Science*, 267(5203), 1512–1515. <https://doi.org/10.1126/science.7878473>
- Lisman, J. E., & Jensen, O. (2013). The theta-gamma neural code. *Neuron*, 77(6), 1002–1016. <https://doi.org/10.1016/j.neuron.2013.03.007>
- Merkow, M. B., Burke, J. F., & Kahana, M. J. (2015). The human hippocampus contributes to both the recollection and familiarity components of recognition memory. *Proceedings of the National Academy of Sciences of the United States of America*, 112(46), 14378–14383. <https://doi.org/10.1073/pnas.1513145112>
- Nyhus, E., & Badre, D. (2015). Memory retrieval and the functional organization of frontal cortex. In D. R. Addis, M. Barense, & A. Duarte (Eds.), *The Wiley handbook on the cognitive neuroscience of memory* (pp. 131–149). Wiley Blackwell. <https://doi.org/10.1002/9781118332634.ch7>
- Nyhus, E., & Curran, T. (2010). Functional role of gamma and theta oscillations in episodic memory. *Neuroscience & Biobehavioral Reviews*, 34(7), 1023–1035. <https://doi.org/10.1016/j.neubiorev.2009.12.014>
- Oostenveld, R., Fries, P., Maris, E., & Schoffelen, J. M. (2011). FieldTrip: Open source software for advanced analysis of MEG, EEG, and invasive electrophysiological data. *Computational Intelligence and Neuroscience*, 2011, 156869. <https://doi.org/10.1155/2011/156869>
- Osipova, D., Takashima, A., Oostenveld, R., Fernandez, G., Maris, E., & Jensen, O. (2006). Theta and gamma oscillations predict encoding and retrieval of declarative memory. *The Journal of Neuroscience*, 26(28), 7523–7531. <https://doi.org/10.1523/JNEUROSCI.1948-06.2006>
- Pacheco Estefan, D., Sánchez-Fibla, M., Duff, A., Principe, A., Rocamora, R., Zhang, H., Axmacher, N., & Verschure, P. F. M. J. (2019). Coordinated representational reinstatement in the human hippocampus and lateral temporal cortex during episodic memory retrieval. *Nature Communications*, 10(1), 2255. <https://doi.org/10.1038/s41467-019-09569-0>
- Pion-Tonachini, L., Kreutz-Delgado, K., & Makeig, S. (2019). ICLabel: An automated electroencephalographic independent component classifier, dataset, and website. *NeuroImage*, 198, 181–197. <https://doi.org/10.1016/j.neuroimage.2019.05.026>
- Polanía, R., Krajčich, I., Grueschow, M., & Ruff, C. C. (2014). Neural oscillations and synchronization differentially support evidence accumulation in perceptual and value-based decision making. *Neuron*, 82(3), 709–720.
- R Core Team. (2021). R: A language and environment for statistical computing. <https://www.R-project.org/>
- Rugg, M. D. (2022). Frontoparietal contributions to retrieval. In M. J. Kahana, & A. D. Wagner (Eds.), *Handbook on Human Memory*. Oxford University Press.
- Staresina, B. P., Michelmann, S., Bonnefond, M., Jensen, O., Axmacher, N., & Fell, J. (2016). Hippocampal pattern completion is linked to gamma power increases and alpha power decreases during recollection. *eLife*, 5, e17397. <https://doi.org/10.7554/eLife.17397>
- Staudigl, T., & Hanslmayr, S. (2013). Theta oscillations at encoding mediate the context-dependent nature of human episodic memory. *Current Biology*, 23(12), 1101–1106.
- Summerfield, C., & Mangels, J. A. (2005). Functional coupling between frontal and parietal lobes during recognition memory. *Neuroreport*, 16(2), 117–122. <https://doi.org/10.1097/00001756-200502080-00008>
- Ursino, M., Cesaretti, N., & Pirazzini, G. (2023). A model of working memory for encoding multiple items and ordered sequences exploiting the theta-gamma code. *Cognitive Neurodynamics*, 17(2), 489–521. <https://doi.org/10.1007/s11571-022-09836-9>
- Wynn, S. C., Daselaar, S. M., Kessels, R. P. C., & Schutter, D. (2019). The electrophysiology of subjectively perceived memory confidence in relation to recollection and familiarity. *Brain and Cognition*, 130, 20–27. <https://doi.org/10.1016/j.bandc.2018.07.003>
- Wynn, S. C., Kessels, R. P., & Schutter, D. J. (2020). Electrocutaneous indices of subjectively perceived confidence in episodic memory. *International Journal of Psychophysiology*, 151, 18–24. <https://doi.org/10.1016/j.ijpsycho.2020.02.007>
- Zhang, Z., Yin, C., & Yang, T. (2022). Evidence accumulation occurs locally in the parietal cortex. *Nature Communications*, 13(1), 4426. <https://doi.org/10.1038/s41467-022-32210-6>

**How to cite this article:** Wynn, S. C., Townsend, C. D., & Nyhus, E. (2024). The role of theta and gamma oscillations in item memory, source memory, and memory confidence. *Psychophysiology*, 61, e14602. <https://doi.org/10.1111/psyp.14602>